RADIATION RESEARCH 65, 1–19 (1976)

Measured Radial Distributions of Dose and LET for Alpha and Proton Beams in Hydrogen and Tissue-Equivalent Gas[1]

CATHARINE L. WINGATE[2] AND JOHN W. BAUM[3]

Health Physics Division, Brookhaven National Laboratory, Upton, New York 11973

WINGATE, C. L., AND BAUM, J. W., Measured Radial Distributions of Dose and LET for Alpha and Proton Beams in Hydrogen and Tissue-Equivalent Gas. *Radiat. Res.* 65, 1–19 (1976).

Experimental measurements of the radial distribution of dose and radially restricted linear energy transfer (L_r) are reported for alpha and proton beams of 1–3 MeV from a Van de Graaff accelerator. The method employs a large cylindrical ionization chamber filled with tissue-equivalent gas (or hydrogen) at variable low pressure for L_r measurement. For radial dose determination, a small movable ionization chamber of transparent mesh located inside the large cylinder is used to measure ionization by secondary electrons around the charged particle beam. Results are presented for simulated tissue radii from about 10 Å to a few thousand angstroms. Comparison of the measured dose distributions with recent calculations by H. G. Paretzke indicates fair agreement except for large radii, where the local energy deposition is a small part of the total.

INTRODUCTION

Spatial distributions of energy deposited radially around charged particle tracks were experimentally determined using ionization chamber techniques and a well-collimated beam of particles. Previous work by Rossi (*1*, *2*), Rossi, Biavati, and Gross (*3*), and others has dealt mainly with event sizes and probability distributions. In the present work a sufficient flux of particles was used to minimize statistical fluctuations. In the measurements by Glass and Roesch (*4*) using a proportional counter, the minimum radius reported was equivalent to 400 Å. Information is needed at smaller radii, such as 20–100 Å, if one is concerned with radiation damage at the molecular or genetic level. We have extended the measurements down to about 10 Å.

An energy-restricted LET, L_Δ, and a radius-restricted LET, L_r, were both defined by the ICRU in 1970 (*5*). That report recommended use of L_Δ when a restricted form of LET is desired. However, large differences between L_Δ and L_r were shown in calculations by Baum (*6*). We believe that L_r restricted to a radius

[1] Research carried out at Brookhaven National Laboratory under contract with the U. S. Atomic Energy Commission.

[2] Present address: Health Sciences Center, State University of New York, Stony Brook, N. Y. 11790.

[3] Send reprint request to J.W.B.

Copyright © 1976 by Academic Press, Inc.
All rights of reproduction in any form reserved.

SCIENCE MUSEUM 12 MAY 76 LIBRARY

of biological interest is more meaningful for radiobiology. Various methods of calculating dose at radius r, D_r, or L_r have been used by Butts and Katz (*7*), Baum, Stone, and Kuehner (*8*), Paretzke and Burger (*9*), Baum (*6*), Chatterjee, Maccabee, and Tobias (*10*), Paretzke (*11*), and Fain, Monnin, and Montret (*12*), but the results differ widely depending on the assumptions made, indicating the need for experimental measurements.

EXPERIMENTAL METHOD

The method involves use of a gas at low pressure in a cylindrical chamber with a beam of charged particles passing on the central axis. Progressive reduction of gas pressure expands the maximum range of secondary electrons. If the maximum range of secondary electrons is less than the chamber radius, the ionization current indicates energy deposition integrated from zero radius to infinite radius, or L_∞. If the maximum range of secondary electrons exceeds the chamber radius, the ionization current indicates L_r, or energy deposition from zero radius to a finite radius which depends on the density of the gas and the chamber dimensions (assuming the contribution by scattered electrons from the chamber wall is negligibly larger than from an infinite gaseous medium). To obtain the dose at radius r, D_r, a small cylindrical ionization chamber (or probe) of almost transparent mesh wall was provided with a mechanism for moving it both radially and axially inside the large chamber. Dose is derived from the ionization current in the probe. The radius, r, is the equivalent distance in condensed medium (unit density tissue or H_2 at 760 Torr) from the beam axis to the probe center.

The large ionization chamber shown in Fig. 1 and used for L_r measurement is an aluminum cylinder, 36 in. long with 12 in. i.d., coated internally with colloidal graphite to ensure conductivity. Voltage is supplied by batteries to this cylinder. The collecting electrode consists of six segments supported on a grounded tube. This permits ion collection from any one of six cylindrical volume segments along the chamber axis and provides a way to check on secondary electron equilibrium and end effects. Ionization current was measured by a vibrating reed electrometer (Victoreen 475) with an accuracy of 1.0%.

The dimensions of the small mesh wall ionization chamber, shown in outline in Fig. 1, are 4.85 in. length, 0.314 in. radius. The mesh in the side and front end walls is made of electroformed nickel wires of 0.0005 in. thickness, 20 wires per inch, giving 97% transparency for particles entering perpendicular to the mesh, or about 92% for isotropic incidence. A copper center wire of 0.028 in. diameter is supported at one end by a Teflon insulator with a grounded guard ring. During observation of current in segments of the large chamber, the probe was placed in a distant segment and no voltage was applied. During use of the probe, all six segment electrodes and the wall of the large chamber were grounded. Collecting voltage was applied to the mesh via external batteries, and the center wire was kept near ground potential since the electrometer requires a low voltage input. Ionization current collected at the center wire was measured by the vibrating reed electrometer. Tests were also conducted with a grounded mesh jacket around the probe. These will be discussed below, in section Chamber Performance and

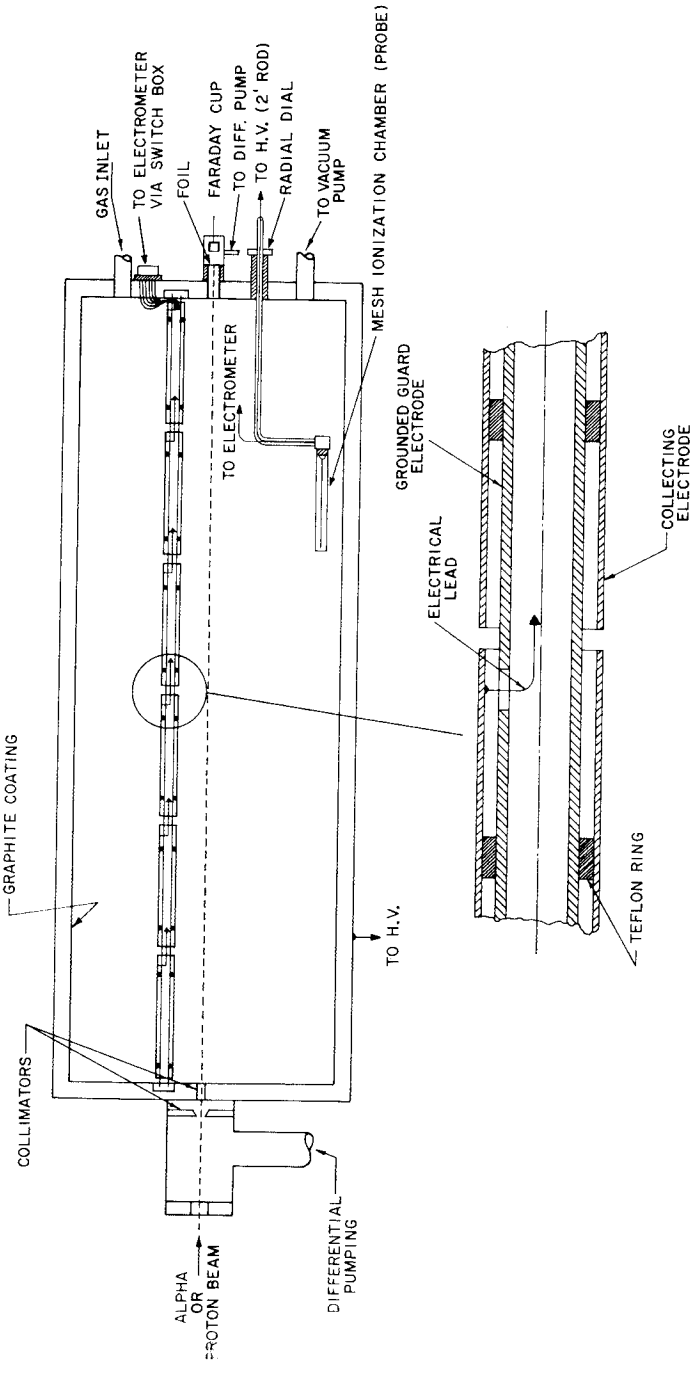

FIG. 1. Schematic diagram of the ionization chambers used.

Special Tests (d). The effective collecting volume of the probe, 23.7 $cm^3 \pm 2\%$, was determined from its dimensions and verified using a radium source of known intensity.

Proton and alpha beams from a Van de Graaff accelerator with nominal energies of 1–3 MeV were used. Actual energies were less than nominal by 0.05 MeV due to machine characteristics. The beam energies were within 2% of the expected value as indicated by a nuclear magnetic resonance probe at the analyzing magnet downstream from the accelerator. Pulse height analysis, using a silicon surface-barrier detector calibrated with an ^{241}Am source, also confirmed the beam energy in the chamber and was used to look for a possible scattered component due to the collimator edge. (See Section f for further details.)

The collimation system is a 0.004 in. diameter hole through a 0.002 in. thick tantalum foil followed, after 0.25 in. separation, by a 0.125 in. diameter tunnel through the aluminum entrance wall of 0.75 in. thickness. The tunnel stops particles scattered through large angles at the foil. A differential pumping section, maintaining pressure at approximately 10^{-5} Torr, precedes the collimator.

The exit beam passed through a nickel foil, 2.5×10^{-5} in. thick, into a copper Faraday cup of 0.75 in. diameter and depth in a brass enclosure evacuated to less than 10^{-4} Torr. The resulting current in the cup, measured by a Keithley electrometer, can be converted to the number of beam particles if their average charge is known. For proton beams the charge is always close to unity. For alpha particles, where electron capture and loss during deceleration are significant, the equilibrium charge for the beam emerging from the foil was taken from the results of Allison (*13*) after calculating the emergent beam energy. For alpha particles of 1 MeV the beam monitoring could not be continuous at pressures of several Torr since much of the beam energy was absorbed in the gas and nickel foil. For this one case, intermittent monitoring was achieved with the Faraday cup by reducing the gas pressure in the chamber temporarily to minimize energy loss in the gas; the beam was stable enough to permit this.

The gases used were (1) a tissue-equivalent mixture (T.E. gas) composed of 64.4% methane, 32.4% carbon dioxide, and 3.2% nitrogen by volume; and (2) hydrogen. Gas flow was regulated by a 20-turn spectrometer leak valve and continuous pumping. Pressure was measured using a Wallace and Tiernan gauge for pressures above 3 Torr and using a Baratron (MKS Instruments, Burlington, Mass.) for pressures below 3 Torr. The latter is an electronic, temperature-regulated device which detects deformation of a metal diaphragm. The response is independent of gas composition and readable to 10^{-4} Torr with an accuracy of 1.0%.

CALCULATION METHOD

The experimentally observed linear energy transfer, L_r, in a segment of the large chamber per beam particle is calculated from the observed quantities using the equation

$$L_r = 10^{-6}\, IW/\rho l n e \qquad (\text{MeV cm}^2/\text{g}), \tag{1}$$

where I is ionization current in the chamber segment in amperes, W is energy per ion pair for the gas and particle beam in electron volts, ρ is gas density in

grams per cubic centimeter, t is the length of a segment in centimeters, e is the electron charge in coulombs, and n is the number of particles traversing the segment per second obtained from the Faraday cup current and the particle charge therein. The value of r is given by $r = \rho d/2$ in grams per square centimeter, where d is the chamber diameter in centimeters (30 cm).

Values of D_r per particle are calculated from the equation

$$D_r = 10^5 I_p W_e F/\rho V n \qquad \text{(rad)}, \tag{2}$$

where I_p is the probe ionization current in amperes, W_e is the energy per ion pair for electrons in the gas, F is a normalization factor for the gas explained below, V is the effective volume of the probe, and other symbols are the same as in Eq. (1), except $r = \rho r_p$ in grams per square centimeter, where r_p is radial distance from the beam to the center of the probe in centimeters provided that r_p exceeds the probe radius, 0.8 cm. (The r_p values used were between 1.2 and 13.8 cm.)

The normalization factor, F, in Eq. (2) is a ratio of gas densities squared but is different for the two gases. The object is to obtain from all data for a single particle, energy, and gas, a single dose distribution curve as a function of radial distance in "tissue" (for T.E. gas) or in hydrogen at atmospheric pressure (for H_2 gas). Thus, the expansion of dimensions achieved by using gas at low pressure is reversed by calculation. If D_r measurements could be made at high gas pressures, the number of secondary electrons produced per unit path of the primary beam would increase proportionally with gas density. Also, the number of electrons intercepted by the probe would increase with gas density since the equivalent radial position would lie closer to the beam and the probe solid angle would be larger as seen by secondary electrons. For a line source (primary beam) this effect varies inversely with radius, or directly with gas density. Combining these effects, the factor F for T.E. gas is $(1/\rho)^2$, since we normalize to unit density. For hydrogen the normalization chosen was to its density at atmospheric pressure and F is $(\rho_a/\rho)^2$, where ρ_a is hydrogen density at 1 atm and 23°C, and ρ is density at the experimental pressure.

The values of W used in Eq. (1) for alpha particles are 31.0 and 36.2 eV/ion pair, in T.E. gas and H_2, respectively. The former is a determination by Kemmochi in this laboratory (1969, unpublished data), the latter is from (*14*). For protons the W value was taken as 1% above the alpha W value, as suggested by Whyte (*14*). The true value of W_e is uncertain due to the large number of low-energy secondary electrons. For simplicity we have assumed W_e equal to W of the beam and constant with energy and, thus, with radial position in the chamber. An alternative assumption, where W_e changes with the mean electron energy, will be discussed below, in section Results and Discussion.

CHAMBER PERFORMANCE AND SPECIAL TESTS

a. Electronic equilibrium. Electronic equilibrium was checked by observing ionization current values for each of the six segments of the large chamber for each beam and gas pressure. The current in the first segment was usually lower than in succeeding segments. Two or more interior segments gave the same current

and were used to determine L_r. The increase along the entire length of the chamber remained less than 4% for T.E. gas at pressure as low as 5×10^{-3} Torr and for hydrogen pressure to 2×10^{-2} Torr. At this T.E. gas pressure, one segment length corresponds to about 10 Å of "tissue," and the chamber length to 60 Å. The short path for equilibrium reflects the fact that most electrons are ejected at 90° to the beam and that an insignificant energy contribution is made by high-energy secondary electrons moving forward. Assuming a straight path for the latter, and classical angles and energies, we calculated a buildup of no more than 5% in the forward direction.

b. Side wall effect. Use of the mesh probe in different positions allowed comparison of dose measurements for a tissue radius simulated by different gas pressures. For example, when the probe is at 12.0 cm radius (near the wall) and pressure is p, the tissue radius is the same as when the pressure is $2p$ and the probe is at 6.0 cm from the beam. If $2p$ is such that secondary electrons (or delta rays) cannot reach the side wall of the big chamber and p is such that they can hit the side wall and possibly cause back-scattered electrons returning to the gas, comparison of results would show any wall effect. No evidence for any significant contribution by back-scattered electrons from the wall to the probe ionization current (saturation value) could be found in numerous comparisons, although this does not exclude the possible presence of very-low-energy back-scattered electrons incapable of ionizing the gas. (See discussion of probe saturation curves below in Part d.)

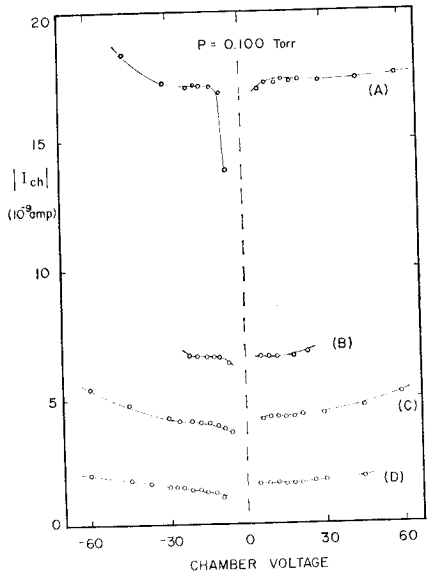

FIG. 2. Ionization current in tissue-equivalent gas in a segment of the large chamber versus voltage applied to the chamber wall. Curve (A) is the 1 MeV alpha particles, p = 0.100 Torr, and chamber radius equivalent to 207 Å tissue. Curve (B) is for 1 MeV protons, p = 0.036 Torr, and chamber radius equivalent to 75 Å tissue. Curve (C) is for 1 MeV alpha particles, p = 0.025 Torr, and chamber radius equivalent to 52 Å tissue. Curve (D) is for 2 MeV alpha particles, p = 0.013 Torr, and chamber radius equivalent to 27 Å tissue.

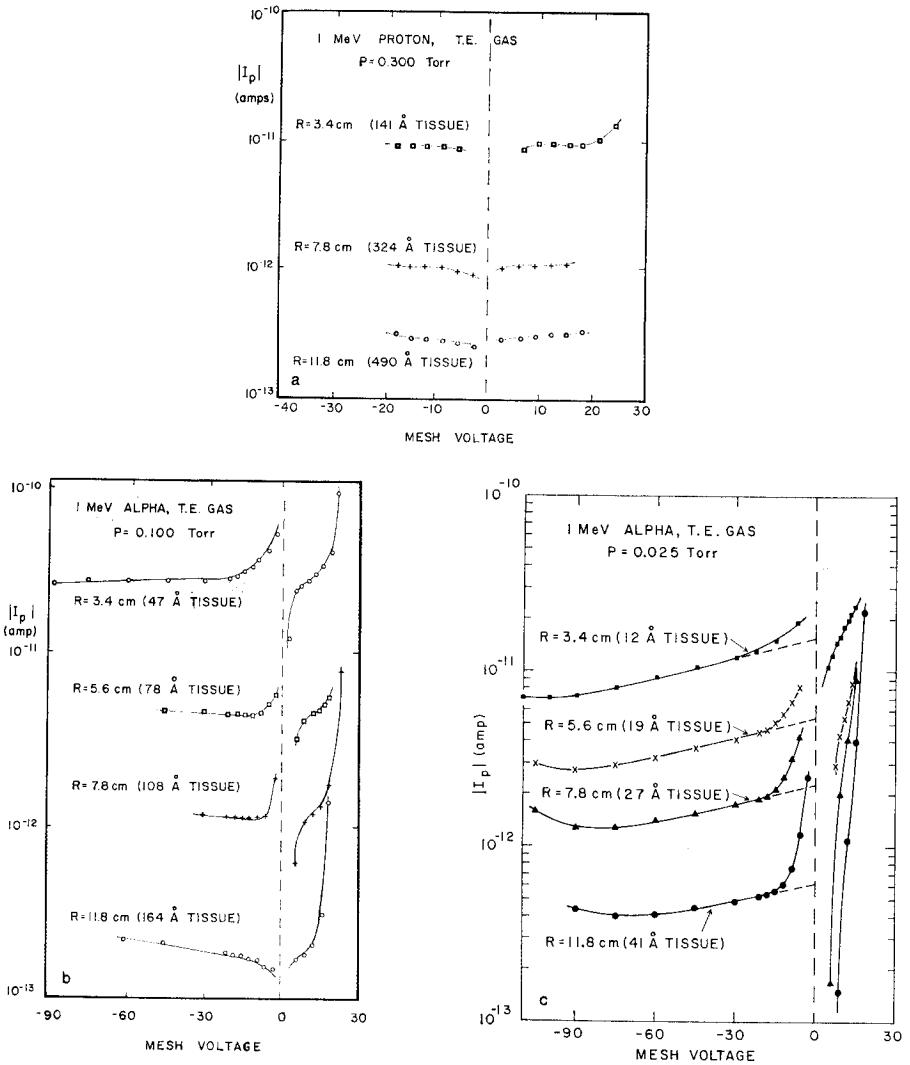

FIG. 3. Probe ionization current in tissue-equivalent gas versus voltage applied to the mesh wall for (a) 1 MeV protons, $p = 0.300$ Torr, (b) 1 MeV alpha particles, $p = 0.100$ Torr, and (c) 1 MeV alpha particles, $p = 0.025$ Torr, for various radial positions of the probe.

c. Chamber saturation curves. Ionization current versus voltage data were obtained for the large chamber for all cases. Representative curves are shown in Fig. 2 for various pressures, particles, and energies. While the plateau region is short at low pressures, there is no difficulty in recognizing a plateau and obtaining an average of positive and negative currents in each case with an uncertainty of less than $\pm 3\%$.

d. Probe saturation curves. For gas pressure about 0.30 Torr (and above) the ionization current-voltage curves for the mesh probe had a normal plateau, as shown in Fig. 3a for 1 MeV protons. Addition of a grounded mesh cylindrical

shield with radius about 0.6 in. did not improve the curve shapes nor significantly change the derived dose.

For lower gas pressures of 0.10 and 0.025 Torr for 1 MeV alphas, shown in Figs. 3b and 3c, the current-voltage curves show several anomalies: (1) In all cases the positive ion current exhibits no plateau, but rather a positive slope. This may be due to acceleration by the electric field of low-energy electrons near the mesh, giving them sufficient energy to produce an ion pair in the collecting volume. (2) For negative ion collection at some probe positions an anomalous high current is exhibited below 10 V instead of the usual buildup. We postulate that his higher-than-plateau current is caused by collection at the center wire of many very-low-energy electrons which enter the probe but lack sufficient energy to ionize the gas or to escape. As larger negative voltages are applied to the mesh, fewer of these low-energy electrons are permitted to enter. This effect disappears as the mesh voltage approaches the ionizing potential of the gas. The ionization produced by secondary electrons is the desired current rather than the secondary electrons themselves. We note that in Fig. 3b the "plateaus" for negative voltage begin at -10 to -15 V and have about the same absolute magnitude as the first inflection point of the positive curve. Thus, when seen together, the positive and negative saturation curves in this case indicate a reasonably unambiguous ionization current. (3) When the corresponding tissue radius is less than 50 Å, a continuing slow decline in current is observed with increasing negative mesh voltage from 10 or 20 V to about 75 V (i.e., more than should be needed for saturation). This suggests the presence of numerous rather low-energy electrons capable of ionizing the gas, which lose significant energy in passing through the mesh or are repelled by it. Therefore, we have extrapolated the slowly declining current to zero volts to remove the decelerating effect of the applied voltage on these electrons, as shown by the dashed lines in Fig. 3c. Current at zero volts is used in Eq. (*2*).

These last two anomalies appear to indicate that the energy spectrum of the secondary electrons varies with radial position. The appearance of a negative current plateau in Fig. 3b when the radial distance to the probe is increased to 78 Å tissue equivalence suggests a changed energy spectrum relative to 47 Å or smaller radii (Fig. 3c). Similarly, the disappearance of the higher-than-plateau current for small negative voltage when the radial distance is increased to 164 Å tissue equivalence suggests that the low-energy electrons have been absorbed at smaller radii and only the more energetic secondary electrons are present.

e. Faraday cup test. The nickel foil used to isolate the Faraday cup from the gas in the experimental chamber introduces the possibility of collecting some electrons emitted from the foil or of scattering some primary particles, giving too low a Faraday cup current and an erroneous indication of beam intensity. To minimize collection of electrons a space of 1.5 in. was left between the foil and the Faraday cup. Tests were also conducted with a deflecting electric field supplied by a metal ring, 1 in. diameter, located between the foil and the Faraday cup. No increase in cup current was obtained with applied voltage. This test does not rule out possible losses due to scattering in the foil for the 1 MeV alpha beam.

f. Collimator scattering and beam energy. The energy spectrum and possible scattering of each beam inside the chamber was studied using a silicon surface

barrier detector (substituted for the Faraday cup) coupled to a multichannel pulse height analyzer. This system was calibrated using an ^{241}Am source for a known energy and a pulse generator for linearity. The beam energies obtained agreed with those from the NMR probe to better than 1%. The width of the energy peak transmitted through the chamber (at less than 10^{-3} Torr pressure) was less than 5% at half-maximum, and except for 3 MeV protons, 90% of the particles were accounted for in the peak. Some of this apparent spread can be attributed to the resolution of the detection system.

In the case of 3 MeV protons a tail of reduced-energy particles was found, amounting to a possible 25% at maximum. This was probably caused by particles which penetrated the tapered edge of the collimator foil. (The hole was produced in the foil by an electric arc.) Thus, data for 3 MeV protons are not as accurate as for 1 and 2 MeV protons. The resulting L_r values could be high at small radii, but L_∞ compares well with published values.

CORRECTIONS

a. Charge exchange. The accelerator delivers singly charged alpha particles which quickly change to doubly charged (approximately) in the gas. From the results of Armstrong *et al.* (*15*), showing that helium ions of energy up to 0.5 MeV reach charge equilibrium in less than 0.1 $\mu g/cm^2$ of gas, we estimated that our alpha beams reached charge equilibrium characteristic of their energy within the first chamber segment for all gas pressures used.

Having achieved charge equilibrium and electronic equilibrium for the majority of secondary electrons, we are now concerned with energy degradation and charge degradation of the beam when higher gas pressures were used. All D_r values for a given beam should refer to the same beam energy and charge in the segment of measurement regardless of gas pressure; otherwise, these data will not lie on a single curve. Since ionization current varies with the square of the charge, the normalizing correction is $(z_e/z_p)^2$, where z_e is the equilibrium charge characteristic of the beam energy reported and z_p is the charge at the higher pressure. The values of z_p were taken from Bichsel's (*16*) tabulation after calculating the arrival energy in the volume segment of observation. The maximum correction was 3% for 1 MeV alpha particles.

b. Scattered beam particles and recoils. Since we assume that the probe ionization current is caused by secondary electrons and since we wish to specify the absorbed dose distribution around a single beam particle, correction is needed for any ions caused in the probe by scattered primary particles or by heavy recoil atoms. From the geometry, primary particles scattered by the first collimator and transmitted through the second collimator (tunnel) could contribute to the probe current only for r_p less than 3 cm. Since the largest radius used was 13.8 cm, much of the probe data did not require correction for scattering at the entrance hole. Data with corrections of more than 25% were discarded unless other substantiating observations at lower pressure (larger r_p) were available.

The effect of gaseous scattering of the primary beam was calculated using the Rutherford elastic scattering equation, substituting N_2 for T.E. gas, and assuming

an average rate of energy loss for the particles and an average path length through the probe. Gaseous scattering was calculated for each particle, energy, gas pressure, and radius. Confirmation of the order of magnitude of beam scattering was obtained using a solid-state detector in various positions inside the chamber for different gas pressures. Scattering corrections were small for most data. Data are given where the scattering contribution approached 50%, when corroborating data with less scatter are also given.

An illustrative example may clarify several points: For 3 MeV alpha particles the dose at a radial distance of about 160 Å of tissue (see Fig. 8c) was obtained with the probe at 11.8 cm from the beam, gas pressure of 0.10 Torr, with a gas scattering contribution of less than 0.1%. The dose was 6.5×10^6 erg/g from this measurement. A neighboring determination was obtained with the probe at 3.4 cm radius from the beam, gas pressure of 0.30 Torr, with a gas scattering contribution of 2% for the same beam. The corresponding radius is 141 Å and the dose was 9.3×10^6 erg/g (higher because it is closer to the beam). A third observation was made with the probe at 1.2 cm radius and 1.00 Torr gas pressure, but now the contribution by primary particles scattered in the gas was about 50% of the observed current, and some particles scattered at the collimator hole may also have contributed ions. The radius was 166 Å and the corrected dose was 5.5×10^6 erg/g. The difference is 17% between the first and third dose values, less 4% for the radial difference, or 13% net.

TABLE I.

LET_∞ (MeV cm²/g)

Particle	*Energy (MeV)*	*Medium*	*Exp. LET values*	*Calculated LET values*					*Ratio Exp./ Avg. Calc.*
				BNL[a]	*UCRL*[b]	*AFWL*[c]	*CEA*[d]	*UCRL*[e]	
Alpha	3	"Tissue"[f]	1180	1277	1200				0.95
	2		1480	1638	1600				0.91
	1		2030	2000	2100				0.99
Alpha	3	H_2	2570	3479			3514		0.74
	2		3870	4736			4764		0.81
	1		5680	6803			7526		0.79
Proton	3	"Tissue"[f]	107	119	120	118		121	0.90
	2		158	160	170	160		164	0.97
	1		266	256	270	264		271	1.01
Proton	3	H_2	297	289		281	298	282	1.04
	2		332	402		392	403	393	0.83
	1		693	683		684	706	676	1.01

[a] Baum (*6*).
[b] Steward and Wallace (*22*).
[c] Janni (*23*).
[d] Williamson, Boujot, and Picard (*24*).
[e] Bichsel (*16*).
[f] Results for several tissue-like materials are included; all experimental values are for T.E. gas, calculated values are all for H_2O except the AFWL values, which are for muscle.

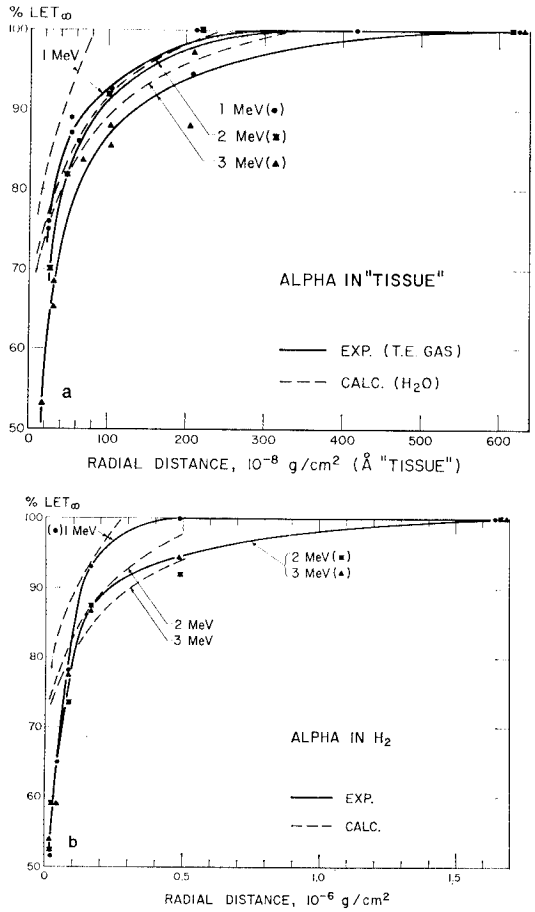

FIG. 4. Radial LET expressed as % LET_∞ for 1–3 MeV alpha particles in (a) tissue-equivalent gas and (b) hydrogen.

Calculations of the contribution to the probe current by recoil nuclei of gas atoms struck by beam particles were also made, again using the Rutherford scattering equation, showing that within the range of the secondary electrons these recoils contribute a negligible amount to the measured current. Thus, no correction is required when comparing to theoretical calculations of dose. For radii greater than the range of secondary electrons, based on classical considerations and published range–energy data (*5*), a few heavy recoils might contribute a small amount of ionization due to their longer range. But electron diffusion or energy straggling could also contribute ionization beyond the expected electron range. We have thus reported values based on the observed current at large radii from the beam without correction for recoils or diffusion.

RESULTS AND DISCUSSION

Table I summarizes the L_∞ results obtained with the large ionization chamber. For evaluation of overall experimental accuracy it also includes calculated L_∞

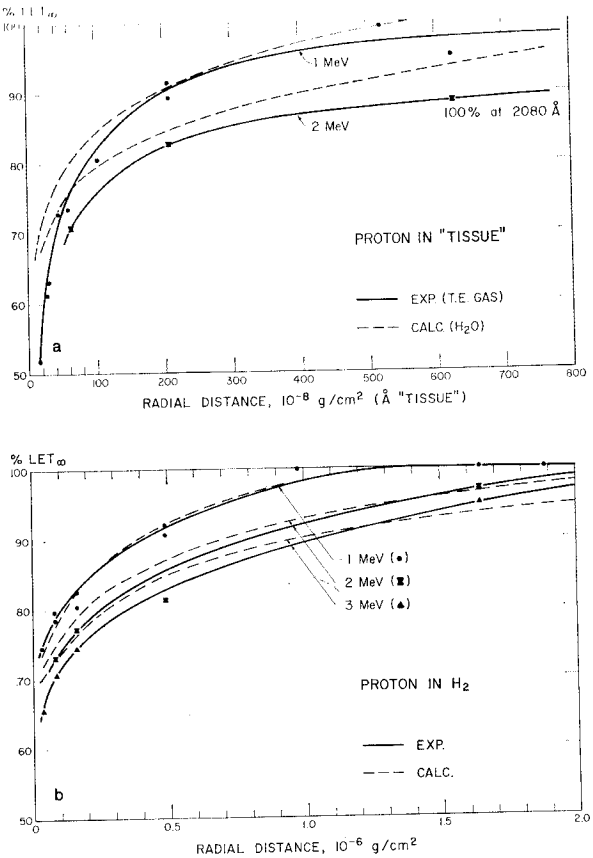

FIG. 5. Radial LET expressed as % LET_∞ for (a) 1 and 2 MeV protons in tissue-equivalent gas and (b) 1–3 MeV protons in hydrogen.

values from five different laboratories. Experimental L_∞ values for alpha particles in H_2 gas were 19–26% lower than the average calculated values. These data may reflect systematic experimental errors caused by possible gas impurity or the difficulty in ascertaining beam constancy when gas pressure is high enough to absorb a large fraction of beam energy before the particles reach the Faraday cup. Since our main interest was in T.E. gas, where L_∞ values were within 12% of the average calculated values, the measurements in H_2 gas were not repeated. Systematic experimental errors tend to cancel when L_r values are normalized or expressed as a fraction of L_∞ as presented below.

Figures 4a, 4b and 5a, 5b show curves of L_r (radially restricted LET) expressed as a fraction of L_∞ versus radial distance for protons and alpha particles in H_2 and in T.E. gas. Dashed curves are calculated values based on Baum's (*6*) model, which employs classical theory of angular and energy distributions of delta rays. Agreement between this theory and experiment is fair for protons and poor for the alpha particles. Less confidence is given results for 1 MeV alpha because of

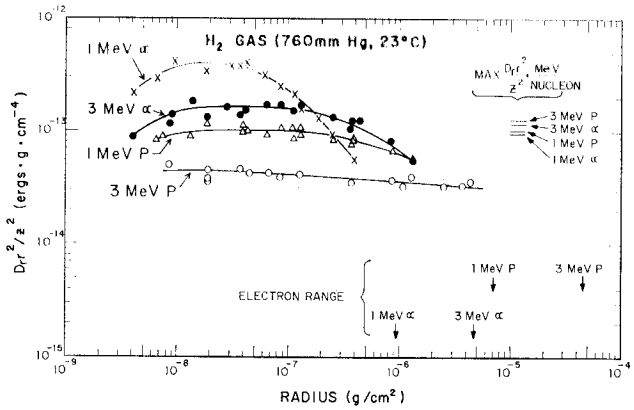

FIG. 6. Dose times radial distance squared divided by z^2 in hydrogen normalized to density at 1 atm and 23°C for alpha and proton beams of 1 and 3 MeV. Arrows at right indicate estimated electron ranges and maximum $D_r r^2/z^2$ times MeV/nucleon. Solid curves are experimental.

uncertainty in assignment of z^2 and uncertainty in interpreting the Faraday cup current (see explanation above in section Experimental Method).

Figures 6 for hydrogen and 7a, 7b for T.E. gas show for all our beams the radial dose determined from the probe current multiplied by r^2/z^2 and plotted against r, where r is radial distance from beam to probe center times gas density (in grams per square centimeter) and z^2 is the effective charge of the beam particles. This greatly condenses the data and allows for convenient comparison. In each of these figures the maximum level of $D_r r^2/z^2$ times MeV/nucleon is also indicated for each beam since these maxima should agree as shown by Paretzke's (*11*) calculations. The alpha maximum levels are low in T.E. gas but the spread of maxima is 17%. Maximum electron ranges estimated from classical energy equations and Cole's (*17*) range data are indicated by arrows on the abscissae of Figs. 6 and 7. The experimental curves bend down toward these range arrows but some ionization was observed beyond the expected cutoff for 1 MeV alpha particles and protons. Calculations by Chatterjee *et al.* (*10*) indicate that electron diffusion could account for the observed dose at large radii and this is consistent with the fact that Cole's measured range was defined to exclude 1% of the ionization produced. Scattering of primary particles at higher gas pressures may also contribute to a broader radial dose distribution than expected. Similar results have been obtained by Varma, Baum, and Kuehner (*18*). For radii less than 20 Å the alpha curves in Fig. 7a decrease unexpectedly. No probable explanation can be offered since overlapping data are not available. For 1 MeV alpha particles and radii below 12 Å a correction of about +30% might be attributable to errors in assumed effective z in the chamber and in the Faraday cup, but this will not remove the downward curvature at small radii completely, nor can so large a correction be applied to 2 and 3 MeV alpha beams. An increased W for electrons would raise the data for small r.

Figures 8 and 9 show semilogarithmic plots of dose versus radial "tissue" distance for alpha and proton beams. The upper distance scale is used to show detail

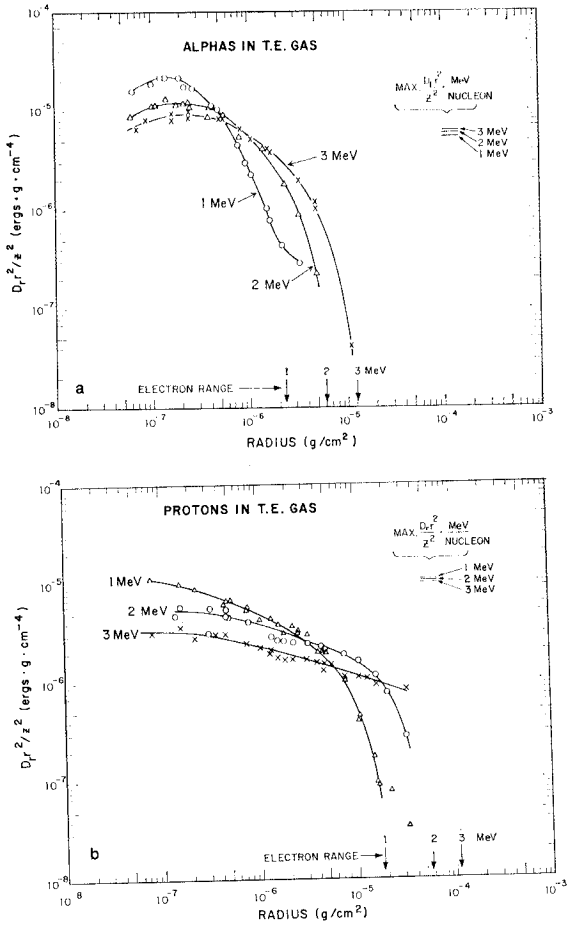

FIG. 7. Dose times radial distance squared divided by z^2 in tissue-equivalent gas normalized to unit density for 1–3 MeV beams of (a) alpha particles and (b) protons. Arrows at right indicate estimated maximum electron ranges and maximum values of $D_r r^2/z^2$ times MeV/nucleon. Solid curves are experimental.

at small radii. Clusters of experimental points represent data taken at different pressures and probe positions. Each curve for a given beam is determined by data points for at least four different experimental pressures indicated by different symbols and four or five probe positions. The scatter of points about the curve reflects nonsystematic errors and is small. (Error bars are not given, since the clustered points are not truly duplicate measurements.) Dashed curves are calculated for water by Paretzke (*11*). His calculations are based on measured spectra of secondary electrons reported by Toburen (*19*, *20*), and the binary encounter theory of Garcia, Gerjuoy, and Welker (*21*). A recent calculation by Fain *et al.* (*12*) also gives reasonable agreement with our results but is not shown here.

We have estimated the effect on D_r of using Cole's (*17*) experimental values of W for low-energy electrons in air. Since W increases as energy decreases for

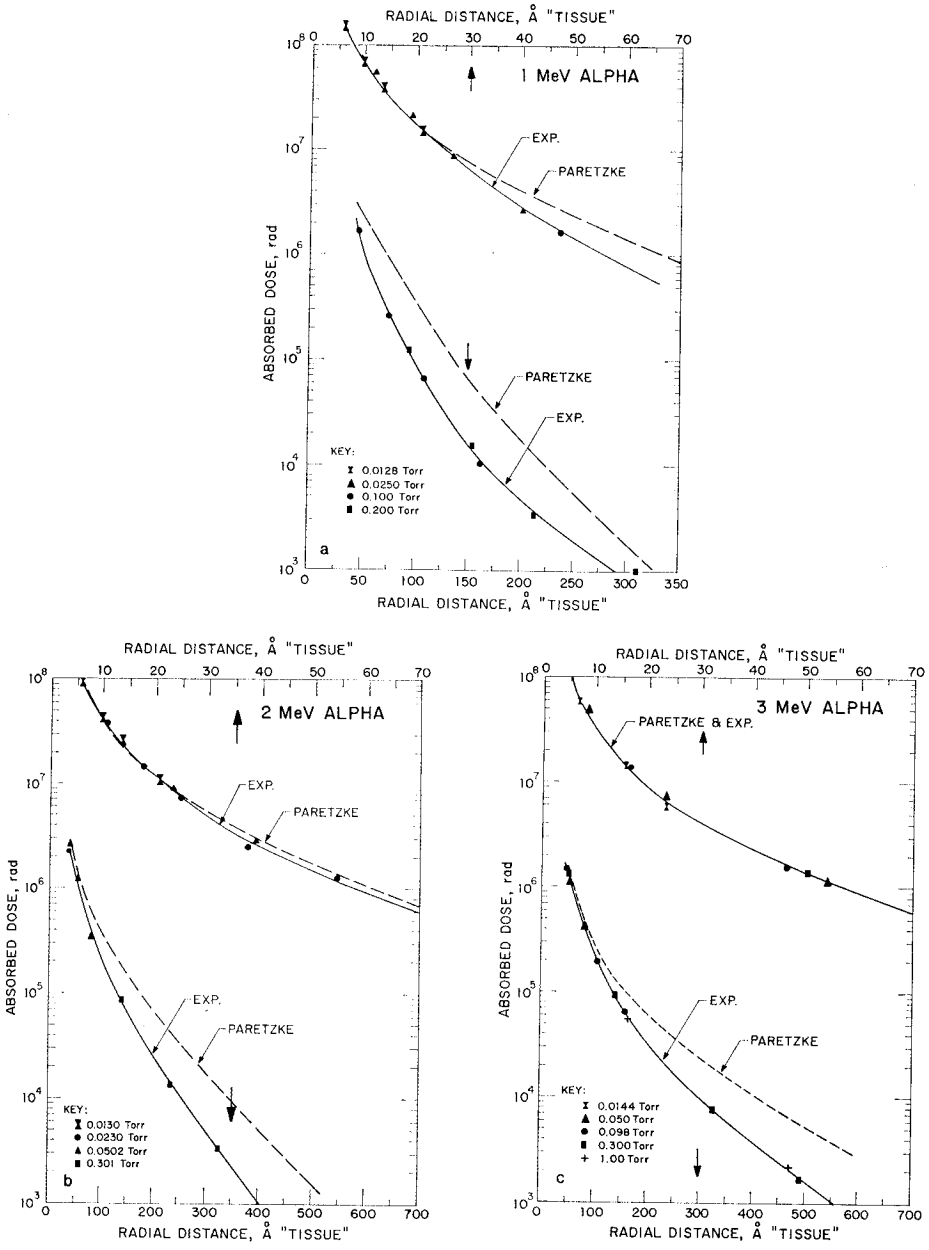

FIG. 8. Experimental dose vs "tissue" radius and calculated curves of Paretzke for alpha particles of (a) 1 MeV, (b) 2 MeV, and (c) 3 MeV. For the upper set of curves the top axis should be read.

low-energy electrons, it is reasonable to expect the average value of W to increase with smaller radial distance. The resulting D_r values for 1 MeV particles would be higher by about 5% at large radii, 10% at 70 Å, and about 60% at 10 Å.

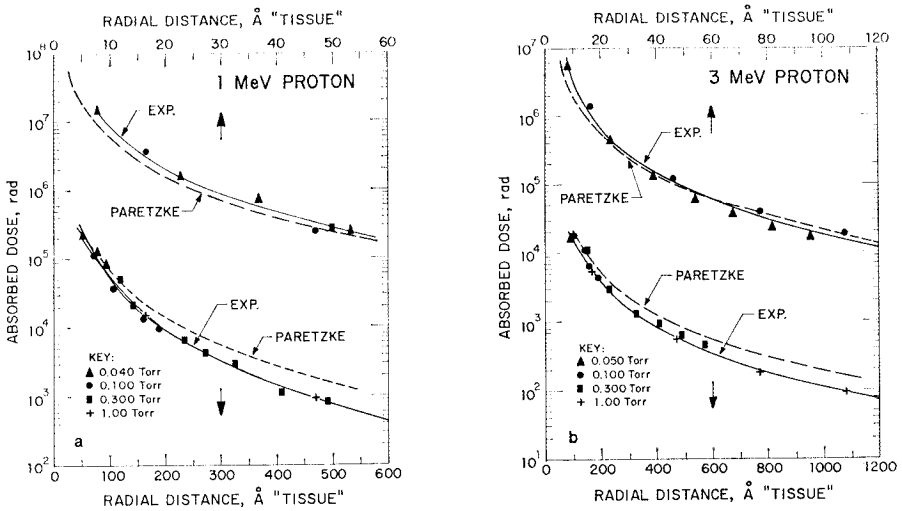

FIG. 9. Experimental dose vs "tissue" radius and calculated curves of Paretzke for protons of (a) 1 MeV and (b) 3 MeV. For the upper set of curves the top axis should be read.

Recent measurements by Waker and Booz (*25*) support the energy dependence of W for electrons at energies below 1 keV. However, the actual magnitude of the W effect on ionization measurements involving many electron energies remains uncertain.

When referring to Figs. 8 and 9, where dose values are very large, it is advisable to keep in mind that any biological target having dimensions of a few angstroms contains very small mass and the resulting mean energy deposition is small. For example, a dose of 10^7 rad would convert to 2.6 eV in a sphere of 10 Å radius. In any irradiation of real tissue the statistics of ionizing events obviously assume great importance.

DISCUSSION OF ERRORS

The observed quantities were measured with the following accuracies: pressure, $\pm 1\%$; electrometer readings, $\pm 2\%$; temperature, $\pm 1\%$; beam energy, $\pm 2\%$. Experimental data in hydrogen were taken at 23°C and an increase of about 8% should be applied when comparing hydrogen results to calculations for 0°C. (This does not apply to results in tissue-equivalent gas corrected to unit density.)

Gas purity is an important consideration when using hydrogen. The gas used was made to specification and tested spectrophotometrically. Tests of out-gas rate of the chamber (after baking) indicated a buildup of about 4×10^{-3} Torr/hr. Most probable impurities are air and hydrocarbon molecules with several times more electrons than hydrogen. The estimated effect of impurities would be to lower the W value by about 3% at most. Frequent flushing and continuous gas flow were employed to minimize this effect. Air leakage or outgassing would have an even smaller effect on the W for T.E. gas. Since tissue-equivalent gas is known to settle into layers of slightly different composition when stored in a vertical tank, the tank was kept horizontal to maintain uniform composition and density.

The correct interpretation of the Faraday cup current depends on knowing the particle charge inside the cup. This is most uncertain in the case of 1 MeV alpha particles because of substantial loss of energy and possible scattering in the nickel foil. We estimate that the number of particles is known to $\pm 3\%$ for all beams except 1 MeV alpha, for which a maximum uncertainty of 30% is possible.

Mention should be made of the uncertainty in the saturation current for the mesh probe at pressures below 5×10^{-2} Torr. (See Fig. 3 and section Chamber Performance and Special Tests (d), above.) We estimate that the extrapolation to zero volts may involve an error of 10–15% for tissue radii below 30 Å. At higher pressures where the saturation curves were normal, the plateau current is known to $\pm 3\%$.

Systematic errors tend to cancel when L_r is normalized to L_∞. Owing to uncertainty in the W value for electrons and the unusual saturation curves, the radial dose calculations must be assigned a larger error than for L_r. There is some justification for using a W_e value of 33.7 eV per ion pair which has been measured for beta rays (*14*), and this would increase all radial dose values in "tissue" by about 8%. The overall experimental error in D_r values for radii greater than 50 Å is estimated as $+20\%$; and for smaller radii, $\pm 40\%$. The overall error in relative L_r values is estimated as half as great for the same radii.

To test the agreement of the results obtained from the two chambers, the probe current data for several beams at a low pressure for all adjacent radial positions including zero radius were multiplied by appropriate volume factors and summed to give an expected ionization current in that segment of the large chamber. Comparison of this sum with the segment current measured in the large chamber agreed within 4% for 1 MeV protons at $\rho = 1$ Torr in H_2, within 2% for 3 MeV alphas at $\rho = 0.10$, 0.05, and 0.005 Torr in T.E. gas, and to about 23% for 1 MeV alpha particles at $\rho = 0.10$ Torr in T.E. gas. This comparison shows good agreement between the two experimental techniques employed as long as unambiguous saturation curves were obtained. D_r measurements, where duplicates were available, indicate reproducibility within 20%.

Agreement with Paretzke's calculated curves is better than 20% for alpha particles at radii less than 30 Å, where more than 95% of the total dose is deposited. For protons in the same radial region the experimental data appear higher than the calculated curve by about 50%. These differences are consistent with our estimate of overall error for small radii. All the experimental curves fall below the theoretical calculations for radii greater than 100 or 200 Å by more than the estimated error. This difference is larger for alpha particles than for protons.

ACKNOWLEDGMENTS

We are grateful for the cooperation of Dr. D. Alburger of the Brookhaven National Laboratory Physics Department, who provided accelerator time and helpful discussions, and of R. Lindgren, operator of the accelerator. We thank Dr. H. Paretzke for providing results of his calculations prior to their publication. We also thank J. Chester, A. Kuehner, and Dr. M. Varma for technical assistance and discussion, and E. Zeidler for machine work.

RECEIVED: July 22, 1974; REVISED: July 25, 1975

REFERENCES

1. H. H. Rossi, Energy distribution in the absorption of radiation. *Adv. Biol. Med. Phys.* **11**, 27–85 (1967).
2. H. H. Rossi, Microscopic energy distribution in irradiated matter. In *Radiation Dosimetry* (F. H. Attix, W. C. Roesch, and E. Tochilin, Eds.), Vol. I, Chap. 2, Academic Press, New York, 1968.
3. H. H. Rossi, M. H. Biavati, and W. Gross, Local energy density in irradiated tissues. *Radiat. Res.* **15**, 431–439 (1961).
4. W. A. Glass and W. C. Roesch, Measurement of ionization distributions in tissue-equivalent gas. *Radiat. Res.* **49**, 477–694 (1972).
5. *Linear Energy Transfer*, ICRU Report 16. International Commission on Radiation Units and Measurements, Washington, D. C., 1970.
6. J. W. Baum, Comparison of distance and energy restricted linear energy transfer for heavy particles with 0.25 to 1000 MeV/amu. *Proc. Second Symposium on Microdosimetry, Stresa, Italy* (H. G. Ebert, Ed.), pp. 653–664. Commission of the European Communities, Brussels, 1970.
7. J. J. Butts and R. Katz, Theory of RBE for heavy ion bombardment of dry enzymes and viruses. *Radiat. Res.* **30**, 855–871 (1967).
8. J. W. Baum, S. L. Stone, and A. V. Kuehner, Radial distribution of dose along heavy ion tracks, LET_r. *Proc. First Symposium on Microdosimetry, Ispra, Italy* (H. G. Ebert, Ed.), pp. 269–291. Commission of the European Communities, Brussels, 1968.
9. H. Paretzke and G. Burger, Spatial distribution of deposited energy along the path of heavy charged particles. *Proc. Second Symposium on Microdosimetry, Stresa, Italy* (H. G. Ebert, Ed.), pp. 615–627. Commission of the European Communities, Brussels, 1970.
10. A. Chatterjee, H. Maccabee, and C. Tobias, Radial cut-off LET and radial cut-off dose calculations for heavy charged particles in water. *Radiat. Res.* **54**, 479–494 (1973).
11. H. G. Paretzke, Comparison of track structure calculations with experimental results. *Proc. Fourth Symposium on Microdosimetry, Verbania Pallanza, Italy* (J. Booz, H. G. Ebert, R. Eickel, and A. Waker, Eds.), pp. 141–165. Commission of the European Communities, Luxembourgh, 1974.
12. J. Fain, M. Monnin, and M. Montret, Spatial energy distribution around heavy-ion path. *Radiat. Res.* **57**, 379–389 (1974).
13. S. K. Allison, Experimental results of charge-changing collisions of hydrogen and helium atoms and ions at kinetic energies above 0.2 keV *Rev. Mod. Phys.* **30**, 1137–1168 (1958).
14. G. N. Whyte, Energy per ion pair for charged particles in gases. *Radiat. Res.* **18**, 265–271 (1973).
15. J. C. Armstrong, J. V. Mullendore, W. R. Harris, ane J. B. Marion, Equilibrium charge-state fractions of 0.2 to 6.5 MeV helium ions in carbon. *Proc. Phys. Soc.* **86**, 1283–1295 (1965).
16. H. Bichsel, Charged particle interactions. In *Radiation Dosimetry* (F. H. Attix, W. C. Roesch, and E. Tochilin, Eds.), Vol. 1, Chap. 4. Academic Press, New York, 1968.
17. A. Cole, Absorption of 20-eV to 50,000-eV electron beams in air and plastic. *Radiat. Res.* **38**, 7–33 (1969).
18. M. N. Varma, J. W. Baum, and A. V. Kuehner, Energy deposition by heavy ions in a tissue equivalent gas. *Radiat. Res.* **62**, 1–11 (1975).
19. L. H. Toburen, Distributions in energy and angle of electrons ejected from molecular nitrogen by 0.3 to 1.7 MeV protons. *Phys. Rev. A* **3**, 216–228 (1971).
20. L. H. Toburen, Energy transfer to electrons in fast proton collisions. *Radiat. Res.* **50**, 6–19 (1972).
21. J. D. Garcia, E. Gerjuoy, and Jean E. Welker, Classical approximation for ionization by proton impact. *Phys. Rev.* **165**, 66–72 (1968).
22. P. G. Steward and R. Wallace, Calculation of stopping power and range-energy values for any heavy ion in nongaseous media. University of California, Lawrence Radiation Laboratory Report, UCRL-17314, 1966.

23. J. F. JANNI, Calculations of energy loss, range, pathlength, straggling, multiple scattering, and the probability of inelastic nuclear collisions for 0.1- to 1000-MeV protons. Air Force Weapons Laboratory Report, AFWL-TR-65-150, 1966.

24. C. F. WILLIAMSON, J. BOUJOT, and J. PICARD, Tables of range and stopping power of chemical elements for charged particles of energy 0.5 to 500 MeV. Commissariat a l'Energie Atomique, Saclay, France, CEA-R 3042, 1966.

25. A. J. WAKER and J. BOOZ, Measurement of the W-value of low energy electrons. *Proc. Second Symposium on Neutron Dosimetry in Biology and Medicine, Neuherberg/Munchen* (G. Burger and H. G. Ebert, Eds.), pp. 455–478. Commission of the European Communities, Luxembourg, 1975.